

Mechanism of Triphosphate Hydrolysis in Aqueous Solution: QM/MM Simulations in Water Clusters

Bella L. Grigorenko, Alexander V. Rogov, and Alexander V. Nemukhin*

Department of Chemistry, M. V. Lomonosov Moscow State University, Moscow, 119992, Russian Federation

Received: November 5, 2005; In Final Form: January 4, 2006

The mechanism of the hydrolysis reaction of the unprotonated methyl triphosphate (MTP) ester in water clusters has been modeled. The effective fragment potential based quantum mechanical–molecular mechanical (QM/MM) approach has been applied in the simulations. It is shown that the minimum energy reaction path is consistent with an assumption of a two-step dissociative-type process similar to the case of the guanosine triphosphate (GTP) hydrolysis in the Ras–GAP protein complex (Grigorenko, B. L.; Nemukhin, A. V.; Topol, I. A.; Cachau, R. E.; Burt, S. K. *Proteins: Struct., Funct., Bioinf.* **2005**, *60*, 495). At the first stage, a unified action of environmental molecular groups and the catalytic water molecule leads to a substantial spatial separation of the γ -phosphate group from the rest of the molecule. At the second stage, inorganic phosphate H_2PO_4^- is formed from water and the metaphosphate anion PO_3^- through the chain of proton transfers along hydrogen bonds. The estimated activation barriers for MTP in aqueous solution at both stages (20 and 14 kcal/mol) are substantially higher than the corresponding barriers for the GTP hydrolysis in the protein.

I. Introduction

The hydrolysis of phosphates is one of the most important chemical processes in biological systems, and therefore its reaction mechanism is a subject of intense modern studies. The main focus of our interest is on modeling guanosine triphosphate (GTP) hydrolysis to guanosine diphosphate (GDP) and inorganic phosphate (Pi) catalyzed by GTP-binding proteins.^{1,2} GTPases regulate biochemical pathways through the ability of GTP/GDP binding proteins for conformational changes depending on the bound species, i.e., GTP or GDP, and the hydrolysis reaction plays a key role in this molecular machinery. Our previous simulations of GTP hydrolysis by the Ras–GAP protein complex performed by using the quantum mechanical–molecular mechanical (QM/MM) theory^{3–10} resulted in a conclusion that the reaction proceeds in two steps basically consistent with the dissociative-type mechanism.² The first step refers to the cleavage of the $\text{O}_\beta\text{--P}_\gamma$ bond and separation of the γ -phosphate group from GDP. This low activation energy process is facilitated by unique positions of the neighboring protein residues and the catalytic water molecule. At the second stage, inorganic phosphate H_2PO_4^- is formed through the chain of proton transfers along hydrogen bonds, also with the low energy transition state.

It is a general belief that modeling a chemical reaction catalyzed by an enzyme should be accompanied by consideration of a similar reaction in aqueous solution in order to clarify the specific function of the protein matrix. Therefore, the main goal of this work was to present the data for the reference system in aqueous solution for a direct comparison to enzymatic conditions. In particular, we intended to learn whether the solvent molecules can furnish similar favorable arrangements of the reagents as in the protein and therefore to precondition the same reaction mechanism as in Ras–GAP.²

In a broader sense, the question of an assignment of the mechanism of the phosphate hydrolysis to either associative or

dissociative type is continuously under debate. The dissociative mechanism assumes the formation of a metaphosphate ion PO_3^- as a reaction intermediate, while in the associative mechanism a pentacoordinated trigonal-bipyramidal phosphorus intermediate plays an essential role. The results of our simulations for the GTP hydrolysis in the Ras–GAP protein complex are basically consistent with the dissociative-type route.²

The conclusions from experimental results¹¹ for the hydrolysis of phosphates in solution have been summarized by Warshel and coauthors.^{12–15} Experimental studies of the hydrolysis of phosphate monoesters in aqueous solution have established a pH dependence of the reaction rate.¹¹ The first-order rate constant decreases from $8 \times 10^{-6} \text{ s}^{-1}$ at pH 4 to $3.5 \times 10^{-6} \text{ s}^{-1}$ at pH 1, and to $1.3 \times 10^{-6} \text{ s}^{-1}$ at pH 7.5 for monomethyl phosphate hydrolysis at 100 °C. For more alkaline solutions, the reaction rate falls below the detection limits. The upper limit for the rate constant of hydrolysis of methyl phosphate dianion (which should be predominant species in solution of phosphate monoesters at pH ~ 7) was set at $5 \times 10^{-8} \text{ s}^{-1}$. Correspondingly, the experimental free energy activation barrier for the hydrolysis of GTP in aqueous solution was estimated as 27.5 kcal/mol on the basis of the rate constant of $5.4 \times 10^{-8} \text{ s}^{-1}$ and traditional transition state theory.¹⁵ On the other hand, Hu and Brink converted the experimental¹¹ rate constant $8 \times 10^{-6} \text{ s}^{-1}$ at pH 4.2 for the methyl phosphate monoanion to the free energy activation barrier of 30.7 kcal/mol at 373 K.¹⁶

From the theoretical side, hydrolysis of phosphates was the subject of several studies by methods of quantum chemistry. An important paper of Ma and coauthors described isomerization of $\text{PO}_3^-\cdot(\text{H}_2\text{O})_n$ clusters to $\text{H}_2\text{PO}_4^-\cdot(\text{H}_2\text{O})_{n-1}$ ($n = 1, 2, 3$).¹⁷ Energy differences between stationary points on potential surfaces were computed by using, in particular, the self-consistent field (SCF) and second-order perturbation theory (MP2) methods. The free energy barriers for isomerization for $n = 1$ were estimated as 32 kcal/mol in the SCF approximation and 22 kcal/mol at the MP2 level by using the DZP + diffuse function basis sets. These barriers were reduced by up to 5 kcal/

* Corresponding author. E-mail: anem@lcc.chem.msu.ru.

mol if the isomerization route included multicenter transition states with the participation of additional ($n = 2, 3$) water molecules.

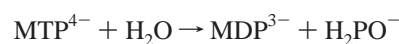
Florián and Warshel¹³ calculated the energy profiles for the methyl phosphate dianion reaction $\text{CH}_3\text{-OPO}_3^{2-} + \text{H}_2\text{O}$ along the assumed associative pathway by using the following strategy: first, the gas-phase transition state geometry configurations and the points along the intrinsic reaction coordinate were obtained at the SCF/6-31G(d) level in the gas phase; second, the energies at these points were recomputed at the MP2/6-31+G(d) level; third, solvation effects were introduced within the Langevin dipole model. Their final estimate for the activation barrier was about 40 kcal/mol.¹³ However, in this model, as well as in the most recent reconsideration of the reaction mechanism of phosphate hydrolysis by Klähn and coauthors,¹⁸ no water molecules from solvation shells were introduced in the system for quantum calculations. Beyond the critical comments on this issue formulated by Hu and Brinck,¹⁶ there is another danger in such an approach. It is known that isolated dianions are generally unstable toward autodetachment (i.e., toward decomposition to monoanion and free electron) and standard quantum chemistry methods cannot be routinely applied for calculation of their potential energy surfaces.¹⁹ Inclusion of a few solvent molecules to the system can remove electronic instability as, for instance, shown experimentally and theoretically for SO_4^{2-} .²⁰

The recent calculations of Akola and Jones²¹ are the most relevant for comparison to our present simulations. These authors modeled the hydrolysis of unprotonated triphosphate methyl ester surrounded by explicit water molecules in the presence of Mg^{2+} by using the Carr–Parrinello molecular dynamics method based on the density functional theory (DFT). They assumed three choices for reaction coordinate in a sense that the chosen geometric parameters were constrained in series of molecular dynamics runs. First, the distance between oxygen O_W from the catalytic water molecule and P_γ was constrained and, as this distance was reduced, the free energy rose gradually to its maximum value of 39.1 kcal/mol at 1.9 Å, corresponding to a pentavalent intermediate of P_γ . Therefore, this route was assigned to the associative mechanism. Second, the $\text{P}_\beta\text{-P}_\gamma$ distance was considered to be a reaction coordinate for a possible dissociative route. When this parameter was increased to 4.5 Å, where the $\text{O}_\beta\text{-P}_\gamma$ bond was broken, the free energy change increased monotonically to 36.6 kcal/mol. In the third choice, the difference of $\text{P}_\beta\text{-P}_\gamma$ and $\text{O}_\text{W}\text{-P}_\gamma$ distances was the reaction coordinate. The free energy reaction barrier obtained in these calculations (35.1 kcal/mol) was assigned to the route along which the $\text{O}_\beta\text{-P}_\gamma$ bond was broken, and after that the nucleophilic attack of water occurred. This way was considered by the authors as the most reasonable, and following an analysis of hydrogen bonding in the system, they subdivided the overall barrier of 35 kcal/mol to 25 kcal/mol required for the $\text{O}_\beta\text{-P}_\gamma$ bond cleavage and the rest to “the artificial stability the PO_3^- metaphosphate resulting from the small size of the sample and the short time scale of simulations.”²¹

In all other theoretical approaches the hydrolysis reaction was modeled by assuming protonated status of the cleaved phosphate group. Florián and Warshel found that for the hydrolysis of the methyl phosphate monoanion the associative and dissociative pathways have close activation barriers.¹³ Hu and Brinck used a variety of quantum chemical methods to calculate the energetics of the associative and dissociative mechanisms for the hydrolysis of the methyl phosphate monoanion.¹⁶ Solvation effects were taken into account by means of a polarizable

continuum model (PCM). According to these calculations, the dissociative mechanism was found to be “strongly” more favorable since along this pathway the calculations resulted in the free energy activation barrier of 29.0 kcal/mol (i.e., within 1.7 kcal/mol discrepancy with their estimate of experimental barrier) versus 38.3 kcal/mol in the associative-type pathway.¹⁶ SCF, MP2, and DFT calculations for methyl phosphate and phenyl phosphate hydrolysis were performed by Mercero et al., resulting in activation free energies for several related species.²² Bianciotto et al.^{23,24} considered dissociative hydrolysis of phosphate monoester monoanions in the presence of one to four water molecules by using DFT and PCM methods. The authors specified the key role of anionic zwitterion $\text{RO}^+(\text{H})\text{PO}_3^{2-}$ intermediate in the reactions. In a recent paper by Wang et al.²⁵ the hydrolysis reactions of monophosphate and triphosphate esters in the gas phase and aqueous solution were studied by using DFT calculations coupled with model solvation approaches. The authors concluded the concurrence of dissociative and associative pathways for the triphosphate ester assuming the protonated status of the γ -phosphate.²⁵

For our purposes, i.e., for the comparison of reaction in solution and in proteins, it is important to consider completely unprotonated phosphate groups. We describe below the results of simulations for the reaction inside water clusters:



where MTP and MDP are methyl triphosphate and methyl diphosphate esters, respectively, performed at the same theoretical level applied before in the case of GTP hydrolysis in the Ras–GAP protein complex.² We use the ab initio type QM/MM method based on the theory of effective fragment potentials,²⁶ and in both applications all phosphate groups, the catalytic water molecule, and the neighboring molecular groups (either side chains of the amino acid residues, or solvent molecules) are assigned to the QM part.

II. The Model and Computational Approaches

The effective fragment potential (EFP) based QM/MM technique is an approach that allows one to perform calculations close to an ab initio treatment of the entire molecular system.²⁶ In this scheme, molecular groups assigned to the MM part are represented by effective fragments that contribute their electrostatic potentials expanded up to octupoles to the quantum Hamiltonian. These one-electron electrostatic potentials as well as contributions from interactions of polarizable effective fragments with the QM region are obtained in preliminary quantum chemical calculations by using ab initio electron densities. The exchange-repulsion potentials to be combined with the electrostatic and polarizability terms are also created in preliminary ab initio calculations. Thus, all empirical parameters are entirely within the MM subsystem. In the original EFP-based approach,²⁶ interactions between solvent molecules are computed as EFP–EFP interactions.²⁷ In our simulations we replaced the EFP–EFP terms by the empirically calibrated TIP3P potentials, which allowed us to formulate a faster computational scheme for large clusters of water molecules around solute species.^{28,29} The computer program created on the basis of the GAMESS³⁰ (more specifically, its Intel-specific version, PC GAMESS³¹) quantum chemistry package and molecular modeling system TINKER³² was used in simulations.

The entire model for QM/MM calculations of energy landscapes included the unprotonated MTP unit surrounded by 81 water molecules. This molecular cluster was created by

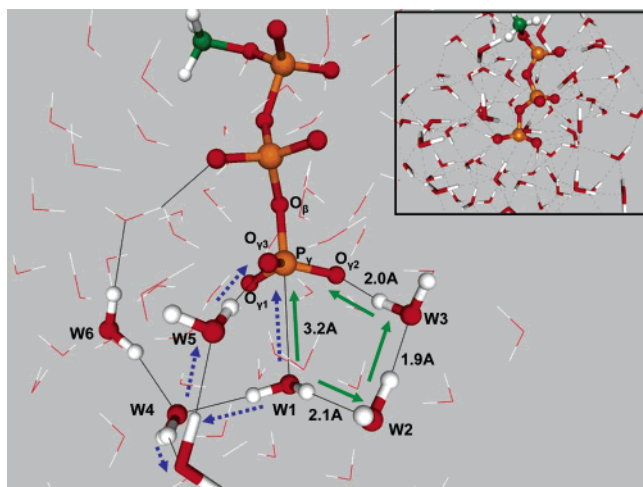


Figure 1. Geometric configuration of the reagents. The inset illustrates a general view of the hydrogen bond network around MTP^{4-} . The arrows indicate possible routes for proton transfers as described in the text.

progressive addition of solvent water molecules (initially all of them considered as effective fragments) and optimizing each time the hydrogen bonded networks within the subsystem until the solute species MTP was completely surrounded by solvent molecules. Analyzing the obtained hydrogen bond networks around MTP (Figure 1), we recognized possible pathways for proton transfers leading from reagents to products and selected six water molecules along this way as active participants that ought to be included in the QM region.

Simulations included scans of the composite multidimensional QM/MM potential energy surface in the regions where chemical bonds or hydrogen bonds could be cleaved or formed. As a result, the basins around presumably stationary points were specified for more careful calculations of the local minima or saddle points. All stationary points considered below were located by unconstrained minimizations (for local minima) or by constrained minimizations (for saddle points) of the QM/MM energy. Locations of the saddle points or, in other words, of transition states were performed basing on the following criterion: the gradient of the constrained internal coordinate along an assumed reaction path must change its sign at this point.

The SCF approximation and the polarized “LANL2DZdp ECP” basis set (and the corresponding pseudopotential for phosphorus)³³ were used in the QM subsystem. It is expected that the energy differences between saddle points and minimum energy points computed at this theoretical level should overestimate activation barriers.

It should be noted that multiple minimum energy points can be located in geometric optimizations for flexible systems such as water clusters which mainly differ by various orientations of solvent molecules. We attempted to overcome this difficulty by performing in each case numerous selections of the starting sets of coordinates for minimization until the lowest energy was reached under the condition that the hydrogen bond network in the immediate vicinity of MTP could be considered perfect.

III. Results

Figure 1 illustrates the equilibrium geometry configuration for the reagents obtained as a minimum energy point. Solid and dashed arrows in Figure 1 indicate two possible pathways for proton transfers along hydrogen bonds leading to the inorganic phosphate, H_2PO_4^- , after cleavage of the $\text{O}_\beta\text{--P}_\gamma$ bond. We

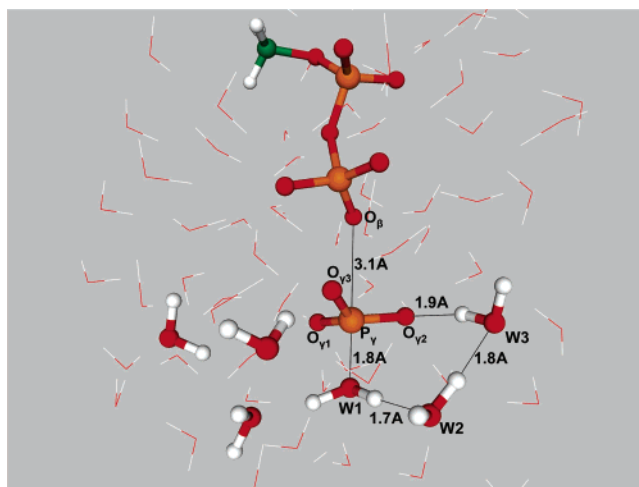
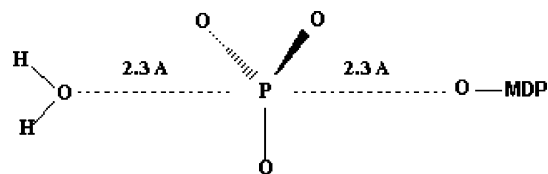


Figure 2. Geometric configuration of the reaction intermediate formed after the stereochemical inversion of the PO_3 group.

considered both these routes and found that the way through the W1, W2, and W3 water molecules (solid arrows) corresponded to lower activation energies in comparison to the path shown by the dashed arrows. In the simulations described below the water molecules W1–W6 were included in the quantum region along with the MTP species.

Apparently, the reagents, W1 and MTP, are aligned in such a fashion that the choice of reaction coordinate for the first stage of reaction is obvious. Three atoms $\text{O}(\text{W1})\text{--P}_\gamma\text{--O}_\beta$ form a line along which the attacking water molecule approaches the γ -phosphate; therefore, we consider the $\text{O}(\text{W1})\text{--P}_\gamma$ distance to be a reaction coordinate. When the $\text{O}(\text{W1})\text{--P}_\gamma$ distance was gradually decreased and all other internal geometric coordinates (including those from the QM part and positions of the solvent molecules as effective fragments) were optimized, the system passed through the potential barrier of 20 kcal/mol and arrived at the configuration of the first intermediate (Figure 2). Remarkably, the $\text{O}_\beta\text{--P}_\gamma$ bond was cleaved at this stage of the reaction, similar to the case of the Ras–GAP protein complex.^{1,2} The configuration of the saddle point (TS1) is characterized by the planar PO_3 group equally distant from the oxygen atoms of the catalytic water and of MDP:



We comment at this point that the choice of reaction coordinate for the phosphate ester hydrolysis as a distance between oxygen from the catalytic water and phosphorus from the γ -phosphate is often considered more appropriate for the associative-type mechanism, for example, in simulations of Akola and Jones.²¹ Following this concept, we also attempted to compute the corresponding energy pathway. By use of two-constrained minimization (for the $\text{O}(\text{W1})\text{--P}_\gamma$ and $\text{O}_\beta\text{--P}_\gamma$ distances), we could estimate the energy profile for such an associative-like reaction; however, the corresponding activation energy was considerably higher than the 20 kcal/mol found for the single-constrained ($\text{O}(\text{W1})\text{--P}_\gamma$) optimization. Therefore, our simulations do not support the associative-type mechanism for hydrolysis of MTP^{4-} in aqueous solution.

In the configuration of the first reaction intermediate (Figure 2), the γ -phosphate unit (metaphosphate) is well separated from

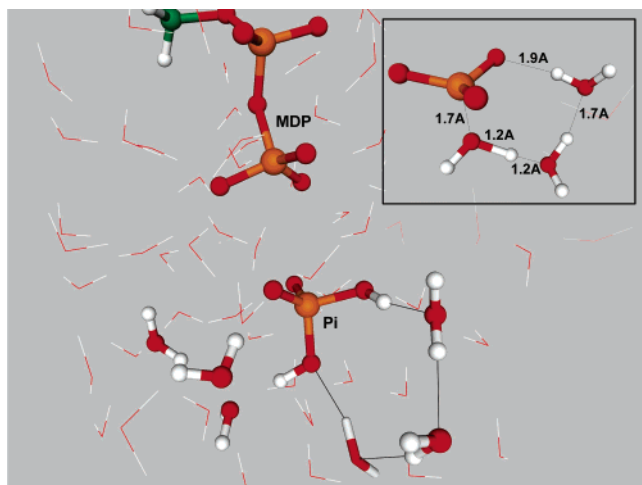


Figure 3. Geometric configuration of the products: $\text{MDP}^{3-} + \text{H}_2\text{PO}_4^-$. The inset shows an arrangement of the atoms in the second transition state TS2.

GDP: the $\text{O}_\beta\text{--P}_\gamma$ distance is 3.1 Å. The next step along the reaction pathway consists of isomerization of $\text{PO}_3^-\cdot(\text{H}_2\text{O})_n$ to $\text{H}_2\text{PO}_4^-\cdot(\text{H}_2\text{O})_{n-1}$ as described computationally for the gas-phase conditions by Ma and coauthors.¹⁷ As mentioned before, we computed the low energy isomerization pathway through the W1--W2--W3 chain of water molecules. This route assumes that the transient H_3O^+ species originating from W2 and W3 finally transferred the proton to $\text{O}_{\gamma 2}$, while the OH^- anion that formed from W1 attacked P_γ . At this stage the elongation of the OH bond in the catalytic water (W1) could serve as the critical degree of freedom. This means that we selected as a reaction coordinate the distance $\text{O}(\text{W1})\text{--H}(\text{W1})$ and all other internal coordinates were adjusted in energy minimization. After successful realization of this approach, we arrived at the configuration of MDP^{3-} and inorganic phosphate H_2PO_4^- (Figure 3). The corresponding saddle point or the second transition state is shown in the inset in Figure 3.

Creation of the H_2PO_4^- species sufficiently modifies the hydrogen bond network around the phosphate tail, which leads to its greater solvation. This observation is consistent with previous knowledge obtained in the calculations of Ma et al.: “the H_2PO_4^- species is about 3 kcal/mol more strongly solvated than either PO_3^- or $\text{PO}_3^-\cdot(\text{H}_2\text{O})$ ” in agreement with the experimental data.¹⁷

IV. Discussion and Conclusions

The main objective of this work was to model the hydrolysis reaction of MTP in aqueous solution and to compare the mechanism to that found before for the GTP hydrolysis in the Ras–GAP protein complex.²

First of all, we notice that the arrangement of key water molecules near the γ -phosphate group of MTP obtained as a result of unconstrained energy minimization for the $\text{MTP}^{4-}\cdot(\text{H}_2\text{O})_{81}$ system (Figure 1) resembles the motifs of the arrangement of key residues in the Ras–GAP protein environment studied before (Figure 4).

For the Ras–GAP catalyzed GTP hydrolysis,² the low activation energy process is facilitated by the unique positions of the neighboring residues—Arg789 from GAP, Gln61, and Thr35 from Ras—as well as of the catalytic water molecule. At the second stage, Gln61 abstracts and releases protons within the subsystem including Gln61, catalytic water, and γ -phosphate, and this transformation also proceeds through the low energy transition state. Figure 4 illustrates the structure of the enzyme–

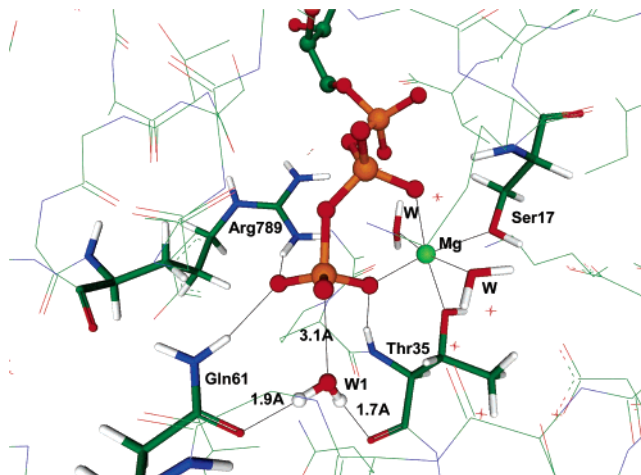


Figure 4. Arrangement of the molecular groups in the active site of the enzyme–substrate complex $\text{H}_2\text{O--GTP--Ras--GAP}$ corresponding to the reagent configuration as obtained in previous QM/MM calculations.²

substrate complex $\text{H}_2\text{O--GTP--Ras--GAP}$, specifying explicitly the active site of the system in the reagent configuration. As shown in Figure 4, the residues Gln61 and Thr35 provide a favorable position of the attacking water molecule (W1) toward the γ -phosphate group accomplished by the hydrogen bond network. In particular, the role of the residues Gln61 and Thr35 is important for the proper orientation of W1. In this position the distance from the negatively charged oxygen atom of water to the positively charged γ -phosphorus of GTP (3.1 Å) is short enough for an efficient interaction of the reagents. The oxygen atoms of the γ -phosphate are captured by Gln61 and Arg789, Thr35 and Mg^{2+} , and Gly60 and Lys16 (not shown in Figure 4), which provides immobility of the reagents, $\text{GTP} + \text{H}_2\text{O}$, in the prereactive state. In such an arrangement the immediate participants of reaction are left with the only degree of freedom to approach each other, namely, along the $\text{O}_\beta\text{--P}_\gamma\text{--O}_\omega$ line. As a result, the $\text{O}_\beta\text{--P}_\gamma$ bond is easily broken already at this stage, leaving the attacking water almost unaltered. After separation of the γ -phosphate from GDP, the stereochemical inversion of the PO_3^- “umbrella” occurs, which allows the catalytic water to approach the metaphosphate ion PO_3^- . As a result, the molecular groups from Gln61, water, and PO_3^- form a cycle within which the protons are transferred until the inorganic phosphate H_2PO_4^- is created.²

Comparing the structure in the protein (Figure 4) and that in the water cluster (Figure 1), we can see similar motifs near the γ -phosphate group. In the aqueous environment, the position of the attacking water molecule W1 toward the γ -phosphate, its orientation by hydrogen bonds with W2 and W4 molecules, and binding of oxygen atoms $\text{O}_{\gamma 1}$ and $\text{O}_{\gamma 2}$ by the neighboring W3 and W5 molecules resemble the arrangement shown in Figure 4.

Therefore, it seems logical that the system modeling the hydrolysis reaction of MTP^{4-} in water clusters evolves through stationary points on the potential energy surface similar to those for the reaction of GTP in the Ras–GAP protein complex. In both cases the reaction is a two-stage process. At the first stage, a unified action of environmental molecular groups and the catalytic water molecule leads to a substantial spatial separation of the γ -phosphate from the rest of the molecule. At the second stage, inorganic phosphate H_2PO_4^- is formed from water and the metaphosphate anion PO_3^- through the chain of proton transfers along hydrogen bonds.

TABLE 1: Relative Energies (kcal/mol) along the Profile Computed for the MTP + H₂O Reaction in Water Clusters in the QM(SCF//LANL2DZdp)/MM(TIP3P) Approximation and for the GTP + H₂O Reaction in the Ras–GAP Protein Complex in the QM(SCF//LANL2DZdp)/MM(AMBER) Approximation (Ref 2)^a

| structure | MTP + H ₂ O in water | GTP + H ₂ O in Ras–GAP |
|--------------|---------------------------------|-----------------------------------|
| reagents | 0.0 | 0.0 |
| TS1 | 20.0 | 4.4 |
| intermediate | 7.0 | −2.0 |
| TS2 | 14.1 | 10.5 |
| products | −20.7 | −9.2 |

^a We note that the relative energies shown in Figure 6 of ref 2 correspond to the values without MM contributions.

In Table 1 we collect the computed total QM/MM energies for the located stationary points obtained in the present work for the MTP + H₂O reaction in water clusters and previously² for the GTP + H₂O reaction in the Ras–GAP protein complex. Such a comparison is justified because qualitatively both model systems evolve through similar stationary points on the respective potential energy surfaces.

The results shown in Table 1 allow us to conclude that the protein matrix facilitates the hydrolysis reaction compared to the aqueous environment due to reduction of the barrier heights at both stages: 4.4 vs 20 kcal/mol for the separation of the metaphosphate anion, and 10.5 vs 14.1 kcal/mol for the creation of inorganic phosphate. Apparently, the qualitative tendency for the energy differences when the aqueous conditions are changed to the protein environment is reproduced. According to the estimates of Shurki and Warshel,³⁴ the experimental free energy activation barrier for the GTP hydrolysis is 27.5 kcal/mol in water and 15.9 kcal/mol in the Ras–GAP protein complex. We compute potential energy barriers of 20 kcal/mol for the relevant reaction in water and 10.5 kcal/mol for the GTP hydrolysis in the protein. The entropic contributions may slightly increase the barriers as, for instance, estimated by Florián and Warshel.¹³

We already mentioned that the energy differences between saddle points and minimum energy points computed at this theoretical level (SCF) should overestimate activation barriers. For instance, in the relevant calculations of Ma and coauthors for the isomerization of PO₃[−](H₂O)_n clusters to H₂PO₄[−](H₂O)_{n−1} (*n* = 1, 2, 3), the following reduction of the barrier height was obtained when the method was changed from SCF to MP2: from 32 to 22 kcal/mol for *n* = 1, from 30 to 21 kcal/mol for *n* = 2, and from 29 to 19 kcal/mol for *n* = 3.¹⁷ In the recent work by the Warshel's group¹⁸ the free activation energy for reaction of metaphosphate with water in solution computed on the basis of the SCF/LANL2DZ method (20 kcal/mol) was almost 2 times higher than that computed in the B3LYP/LANL2DZ approximation (11 kcal/mol). Our estimates of the contributions from electron correlation effects were on the same order: when we repeated single point calculations for the reagent configuration and for the first transition state in the MP2/LANL2DZ//SCF/LANL2DZ approximation, the activation energy decreased to 11 from 20 kcal/mol. However, we do not believe that such an approach based on single point estimates at the stationary points located in the SCF calculations is a trustworthy way to incorporate correlation effects, and the better strategy would be geometric optimization at the higher level.

By all means, in this and in previous² simulations we succeeded in describing the low-energy routes from reagents (triphosphate and water) to products (diphosphate and inorganic phosphate) with activation barriers not exceeding 20 kcal/mol for aqueous solution and 10 kcal/mol for the Ras–GAP protein complex. In all previous quantum based calculations^{16,21–25} these

quantities were substantially higher (close to 30 kcal/mol). We wrote before that the Carr–Parrinello molecular dynamics simulations by Akola and Jones²¹ are the most relevant for comparison to our approach in the sense that the completely unprotonated MTP species are considered in their and our modeling. Protonation of one of the oxygen atoms in the γ -phosphate group should lead to considerably different conditions for the reaction flow and to increasing the activation barriers due to partial reduction of electrostatic repulsion of the phosphate units. However, the barriers reported by Akola and Jones were considerably higher, i.e., about 35 kcal/mol, although the authors somehow justified the lower value (25 kcal/mol) for the O _{β} –P _{γ} bond cleavage.²¹ From the qualitative side, the conclusions of our simulations and of those of ref 21 are fairly similar, favoring the dissociative type of the reaction mechanism. We believe that the QM/MM modeling described in the present work provides more a detailed mechanistic picture of the chemical events and supplies the appropriate reference data for comparison to the enzymatic reaction. We think that for other enzymes catalyzing nucleoside triphosphate hydrolysis we shall recognize the motifs with the key amino acid residues resembling the arrangement of water molecules responsible for the MTP hydrolysis in aqueous solutions.

Note Added in Proof. In a recent paper (Koetting, C.; Gerwert, K. *Chem. Phys.* **2004**, 307, 227) the authors reported the measured activation energy of GTP hydrolysis in an aqueous solution of 26 kcal/mol.

Acknowledgment. We thank Prof. A. Warshel, Dr. I. Topol, and Dr. S. Burt for stimulating discussions on the subject. This work is supported in part by a grant from the Russian Foundation for Basic Researches (Project No. 04-03-32008).

References and Notes

- Topol, I. A.; Cachau, R. E.; Nemukhin, A. V.; Grigorenko, B. L.; Burt, S. K. *Biochim. Biophys. Acta* **2004**, 1700, 125.
- Grigorenko, B. L.; Nemukhin, A. V.; Topol, I. A.; Cachau, R. E.; Burt, S. K. *Proteins: Struct., Funct., Bioinf.* **2005**, 60, 495.
- Warshel, A.; Levitt, M. *J. Mol. Biol.* **1976**, 103, 227.
- Field, M. J.; Bash, P. A.; Karplus, M. *J. Comput. Chem.* **1990**, 11, 700.
- Gao, J. L. *Acc. Chem. Res.* **1996**, 29, 298.
- Shoemaker, J. R.; Burggraf, L. W.; Gordon, M. S. *J. Phys. Chem. A* **1999**, 103, 3445.
- Monard, G.; Merz, K. M. *Acc. Chem. Res.* **1999**, 32, 904.
- Murphy, R. B.; Philipp, D. M.; Friesner, R. A. *J. Comput. Chem.* **2000**, 21, 1442.
- Zhang, Y.; Liu, H.; Yang, W. *J. Chem. Phys.* **2000**, 112, 3483.
- Cui, Q.; Elstner, M.; Kaxiras, E.; Frauenheim, T.; Karplus, M. *J. Phys. Chem. B* **2001**, 105, 569.
- Bunton, C. A.; Llewellyn, D. R.; Oldham, K. G.; Vernon, C. A. *J. Chem. Soc.* **1958**, 3574.
- Florián, J.; Warshel, A. *J. Am. Chem. Soc.* **1997**, 119, 5473.
- Florián, J.; Warshel, A. *J. Phys. Chem. B* **1998**, 102, 719.
- Åqvist, J.; Kolmodin, K.; Florián, J.; Warshel, A. *Chem. Biol.* **1999**, 6, R71.
- Glennon, T. M.; Villa, J.; Warshel, A. *Biochemistry* **2000**, 39, 9641.
- Hu, C. H.; T. Brinck, T. J. *Phys. Chem. A* **1999**, 103, 5379.
- Ma, B. Y.; Xie, Y. M.; Shen, M. Z.; Schleyer, P. V.; Schaefer, H. F. *J. Am. Chem. Soc.* **1993**, 115, 11169.
- Klähn, M.; Braun-Sand, S.; Rosta, E.; Warshel, A. *J. Phys. Chem. B* **2005**, 109, 15645.
- Dreuw, A.; Cederbaum, L. S. *Chem. Rev.* **2002**, 102, 181.
- Wang, X.-B.; Nicholas, J. B.; Wang, L.-S. *J. Chem. Phys.* **2000**, 113, 10837.
- Akola, J.; Jones, R. O. *J. Phys. Chem. B* **2003**, 107, 11774.
- Mercero, J. M.; Barrett, P.; Lam, C. W.; Fowler, J. E.; Ugalde, J. M.; Pedersen, L. G. *J. Comput. Chem.* **2000**, 21, 43.
- Bianciotto, M.; Barthelat, J. C.; Vigroux, A. *J. Phys. Chem. A* **2002**, 106, 6521.
- Bianciotto, M.; Barthelat, J. C.; Vigroux, A. *J. Am. Chem. Soc.* **2002**, 124, 7573.

- (25) Wang, Y. N.; Topol, I. A.; Collins, J. R.; Burt, S. K. *J. Am. Chem. Soc.* **2003**, *125*, 13265.
- (26) Gordon, M. S.; Freitag, M. A.; Bandyopadhyay, P.; Jensen, J. H.; Kairys, V.; Stevens, W. J. *J. Phys. Chem. A* **2001**, *105*, 293.
- (27) Merrill, G. N.; Webb, S. P. *J. Phys. Chem. A* **2004**, *108*, 833.
- (28) Nemukhin, A. V.; Grigorenko, B. L.; Topol, I. A.; Burt, S. K. *Phys. Chem. Chem. Phys.* **2004**, *6*, 1031.
- (29) Dobrogorskaia-Mereau, Ia. I.; Nemukhin, A. V. *J. Comput. Chem.* **2005**, *26*, 865.
- (30) Schmidt, M. W.; Baldrige, K. K.; Boatz, J. A.; Elbert, S. T.; Gordon, M. S.; Jensen, J. H.; Koseki, S.; Matsunaga, N.; Nguyen, K. A.; Su, S. J.; Windus, T. L.; Dupuis, M.; Montgomery, J. A. *J. Comput. Chem.* **1993**, *14*, 1347.
- (31) Granovsky, A. A. <http://lcc.chem.msu.ru/gran/gameess/index.html>.
- (32) Ponder, J. <http://dasher.wustl.edu/tinker>.
- (33) Hay, P. J.; Wadt, W. R. *J. Chem. Phys.* **1985**, *82*, 270.
- (34) Shurki, A.; Warshel, A. *Proteins: Struct., Funct., Bioinf.* **2004**, *55*, 1.